

AN ENTROPIC FOURIER METHOD FOR THE BOLTZMANN EQUATION

ZHENNING CAI*, YUWEI FAN[†], AND LEXING YING[‡]

Abstract. We propose an entropic Fourier method for the numerical discretization of the Boltzmann collision operator. The method, which is obtained by modifying a Fourier Galerkin method to match the form of the discrete velocity method, can be viewed both as a discrete velocity method and as a Fourier method. As a discrete velocity method, it preserves the positivity of the solution and satisfies a discrete version of the H-theorem. As a Fourier method, it allows one to readily apply the FFT-based fast algorithms. A second-order convergence rate is validated by numerical experiments.

Key words. Fourier method; discrete velocity method; Boltzmann equation; modified Jackson filter; H-theorem; positivity.

AMS subject classifications. 65M70, 65R20, 76P05

1. Introduction. Gas kinetic theory describes the statistical behavior of a large number of gas molecules in the joint spatial and velocity space. It has been widely used to model gases outside the hydrodynamic regime, for example in the field of rarefied gas dynamics. Let $f(t, x, v)$ be the mass density distribution of the particles, depending on the time $t \in \mathbb{R}^+$, position $x \in \mathbb{R}^d$ ($d \geq 2$) and microscopic velocity $v \in \mathbb{R}^d$. Based on the molecular chaos assumption, the Boltzmann equation

$$(1.1) \quad \frac{\partial f}{\partial t} + v \cdot \nabla_x f = \mathcal{Q}[f, f], \quad f(0, x, v) = f^0(x, v)$$

for the evolution of $f(t, x, v)$ was derived in [6] and has served as the fundamental equation in the gas kinetic theory. When modeling the binary interaction between the particles, the Boltzmann collision operator $\mathcal{Q}[f, f]$ takes the form

$$(1.2) \quad \mathcal{Q}[f, f](v) = \int_{\mathbb{R}^d} \int_{\mathbb{S}^{d-1}} \mathcal{B}(v - v_*, \omega) [f(v')f(v'_*) - f(v)f(v_*)] dv_* d\omega$$

for monatomic gases, where

$$v' = \frac{v + v_*}{2} + \frac{|v - v_*|}{2} \omega, \quad v'_* = \frac{v + v_*}{2} - \frac{|v - v_*|}{2} \omega$$

are the post-collisional velocities of two particles with pre-collisional velocities v and v_* , and ω is the angular parameter of the collision. Here the variables t and x are omitted for simplicity and we shall continue doing so when focusing only on the collision term. The collision kernel \mathcal{B} is non-negative and usually takes the form

$$(1.3) \quad \mathcal{B}(v - v_*, \omega) = b(|v - v_*|, \cos \theta), \quad \cos \theta = |(v - v_*) \cdot \omega| / |v - v_*|.$$

The Boltzmann equation (1.1) guarantees that $f(t, x, v)$ remains non-negative if the initial value $f(t = 0, x, v)$ is also non-negative [28]. The symmetry of the collision

*Department of Mathematics, National University of Singapore, Singapore 119076 (matcz@nus.edu.sg).

[†]Department of Mathematics, Stanford University, Stanford, CA 94305 (ywf@stanford.edu).

[‡]Department of Mathematics and Institute for Computational and Mathematical Engineering, Stanford University, Stanford, CA 94305 (lexing@stanford.edu).

term (1.2) and the fact $dv dv_* = dv' dv'_*$ imply that for any function $\psi(\cdot)$:

$$(1.4) \quad \int_{\mathbb{R}^d} \psi(v) \mathcal{Q}[f, f](v) dv = \frac{1}{4} \int_{\mathbb{R}^d} \int_{\mathbb{R}^d} \int_{\mathbb{S}^{d-1}} (\psi(v) + \psi(v_*) - \psi(v') - \psi(v'_*)) \mathcal{B}[f(v')f(v'_*) - f(v)f(v_*)] dv_* dv d\omega.$$

Setting $\psi(v) = 1, v, |v|^2$ gives rise to the conservation of the mass, momentum and energy

$$(1.5) \quad \int_{\mathbb{R}^d} \mathcal{Q}[f, f](v) dv = 0, \quad \int_{\mathbb{R}^d} \mathcal{Q}[f, f](v)v dv = 0, \quad \int_{\mathbb{R}^d} \mathcal{Q}[f, f](v)|v|^2 dv = 0,$$

respectively. The famous H-theorem that states the monotonicity of the entropy

$$(1.6) \quad \int_{\mathbb{R}^d} \mathcal{Q}[f, f](v) \ln(f(v)) dv = \frac{1}{4} \int_{\mathbb{R}^d} \int_{\mathbb{R}^d} \int_{\mathbb{S}^{d-1}} \ln\left(\frac{f(v)f(v_*)}{f(v')f(v'_*)}\right) \mathcal{B}[f(v')f(v'_*) - f(v)f(v_*)] dv_* dv d\omega \leq 0$$

can also be obtained by setting $\psi(v) = \ln(f(v))$.

By introducing new variables $y = v' - v$ and $z = v'_* - v$ and carrying out algebra calculations, the Boltzmann collision operator can be rewritten as (see [7, 22, 19] for details)

$$(1.7) \quad \mathcal{Q}[f, f](v) = \int_{\mathbb{R}^d} \int_{\mathbb{R}^d} \tilde{\mathcal{B}}(y, z) \delta(y \cdot z) [f(v+y)f(v+z) - f(v)f(v+y+z)] dy dz.$$

This is the well-known Carleman representation [7] of the Boltzmann collision operator, where $\tilde{\mathcal{B}}(y, z)$ is related to $\mathcal{B}(v - v_*, \omega)$ in (1.3) by

$$(1.8) \quad \tilde{\mathcal{B}}(y, z) = 2^{d-1} \mathcal{B}\left(y + z, \frac{y - z}{|y - z|}\right) |y + z|^{2-d}.$$

Though the Boltzmann equation serves as the fundamental equation in gas dynamics, its high dimensional nature and the complexity of the collision operator pose difficulties for its numerical solution. A classical method is the direct Monte Carlo simulation [2], which uses simulated particles to mimic gas molecules and handles the collisions in a stochastic way. Though it treats the high dimensionality effectively, the convergence order is low and the numerical solution appears rather oscillatory.

With the rapid growth of computing power, it has become more practical to solve the Boltzmann equation with deterministic methods. For all deterministic approaches, the complexity of the collision integral poses the most serious difficulty for numerical computation. Therefore, this paper focuses on the spatially homogeneous case

$$(1.9) \quad \frac{\partial f}{\partial t} = \mathcal{Q}[f, f]$$

for simplicity.

In the past decades, several deterministic schemes have been developed for the Boltzmann collision term. Two methods that have attracted the most attention are the discrete velocity method (DVM) [13, 27, 4, 22] and the Fourier Galerkin method (FGM) [5, 23, 24], which will be reviewed in what follows.

1.1. Discrete velocity method. The discrete velocity method (DVM) assumes that the particle velocity takes only values from a finite set. Consider a domain $\mathcal{D}_T = [-T, T]^d$ for the velocity variable v , that is discretized uniformly with step size $h = 2T/N$ for a positive integer N (which is assumed to be odd for simplicity). By adopting the d -dimensional multi-index notation $k = (k_1, \dots, k_d)$, one can denote the set of discrete velocity samples by

$$(1.10) \quad X = \{h \cdot k \mid k = (k_1, \dots, k_d), -n \leq k_1, \dots, k_d \leq n\}.$$

where $N = 2n + 1$. In the rest of this paper, we use the lower-case letters p, q, r and s to denote the discrete velocity samples in X .

Using $F_r(t)$ for $r \in X$ as the numerical approximations of the distribution function $f(t, v)$ at the points in X , the governing equations of DVM for $F_r(t)$ are

$$(1.11) \quad \frac{dF_r(t)}{dt} = Q_r(t) := \sum_{p, q, s \in X} A_{pq}^{rs} (F_p(t)F_q(t) - F_r(t)F_s(t)), \quad r \in X.$$

Here $Q_r(t)$ serves as an approximation to $\mathcal{Q}[f, f](t, r)$. The coefficients A_{pq}^{rs} are non-negative constants and satisfy the conservation relations

$$(1.12) \quad A_{pq}^{rs} \neq 0 \quad \Rightarrow \quad p + q = r + s \quad \text{and} \quad |p|^2 + |q|^2 = |r|^2 + |s|^2$$

and the symmetry property

$$(1.13) \quad A_{pq}^{rs} = A_{qp}^{rs} = A_{rs}^{pq}.$$

The property (1.12) shows that the collisions in DVM also satisfy the momentum and energy conservation, and the property (1.13) implies that the collisions are also reversible as in the Boltzmann equation. These two facts guarantee that DVM maintains a number of fundamental physical properties of the continuous Boltzmann equation, such as (a) the positivity of the distribution function, (b) the exact conservation of mass, momentum and energy, and (c) a discrete H-theorem.

More precisely, the values $F_r(t)$ for $r \in X$ are always non-negative if the initial values $F_r(t=0)$ are non-negative [28, 26]. The symmetry relation (1.13) implies that

$$(1.14) \quad \sum_{r \in X} Q_r \psi_r = \frac{1}{4} \sum_{p, q, r, s \in X} A_{pq}^{rs} (\psi_r + \psi_s - \psi_p - \psi_q) (F_p F_q - F_r F_s).$$

Combining (1.14) and the relations (1.12) gives rise to the conservation of mass, momentum and energy in the discrete sense

$$(1.15) \quad \sum_{r \in X} Q_r = 0, \quad \sum_{r \in X} Q_r r = 0, \quad \sum_{r \in X} Q_r |r|^2 = 0.$$

After letting $\psi_r = \ln(F_r)$ in (1.14), one obtains a discrete version of the H-theorem for DVM

$$(1.16) \quad \sum_{r \in X} Q_r \ln(F_r) = \frac{1}{4} \sum_{p, q, r, s \in X} A_{pq}^{rs} \ln \left(\frac{F_r F_s}{F_p F_q} \right) (F_p F_q - F_r F_s) \leq 0$$

using the non-negativity of the coefficients A_{pq}^{rs} and the monotonicity of the \ln function. Notice that, in this argument, the symmetry relations (1.13), the non-negativity of

A_{pq}^{rs} , and the non-negativity of the initial values are all essential for derivation of the H-theorem.

As a direct discretization for the high-dimensional integral of the collision term, DVM has a rather high computational cost $O(N^{2D+\delta})$ for some $0 < \delta \leq 1$ [8]. It is also difficult to achieve decent convergence rate due to the insufficiency collision pairs in the Cartesian grid used for velocity discretization. More precisely, in the 2D case, the rate of convergence of DVM introduced in [13] is only $O((1/\log h)^p)$ with $p < 1/2 - 1/\pi$ [9]. For the 3D case, the best rate of convergence of DVM is also slower than the first order [21, 22].

The method in [18, 29] tries to improve the accuracy of DVM by interpolation. While the mass, momentum and energy are conserved in this scheme, positivity and the H-theorem fail to hold. The fast algorithm in [20] reduces the computational cost of DVM to $O(\bar{N}^d N^d \log(N))$ with some parameter $\bar{N} \ll N$ for the hard sphere molecules, but it abandons the conservation of momentum and energy.

1.2. Fourier Galerkin method. The Fourier-based methods assume that the distribution function $f(t, v)$ is supported (in the v variable) in a ball $B_{R/2}$ centered at the origin with radius $R/2$. Under this assumption, it makes sense to focus on the functions $f(t, v)$ with $\text{Supp}(f) \subset B_{R/2}$. For those functions, $\text{Supp}(\mathcal{Q}[f, f]) \subset B_{\sqrt{2}R/2}$ and the collision term $\mathcal{Q}[f, f]$ reduces to a truncated version $\mathcal{Q}^R[f, f]$ defined as

$$(1.17) \quad \mathcal{Q}^R[f, f](v) := \int_{B_R} \int_{B_R} \tilde{\mathcal{B}}(y, z) \delta(y \cdot z) [f(v+y)f(v+z) - f(v)f(v+y+z)] dy dz,$$

where the superscript in $\mathcal{Q}^R[f, f]$ denotes the truncation radius. In order to obtain a spectral approximation to the collision term, one restricts the domain of the distribution function $f(v)$ to the cube $\mathcal{D}_T = [-T, T]^d$ with $T \geq \frac{3\sqrt{2}+1}{4}R$ in order to reduce aliasing. One then extends it periodically to the whole space. (See [24, 19] for details of the derivation). After periodization, $f(v)$ can be written as a Fourier series

$$(1.18) \quad f(v) = \sum_{k \in \mathbb{Z}^d} \hat{f}_k E_k(v), \quad \hat{f}_k = \frac{1}{(2T)^d} \int_{\mathcal{D}_T} f(v) E_{-k}(v) dv,$$

where $E_k(v) = \exp(\frac{i}{T}k \cdot v)$. Substituting (1.18) into (1.17) gives rise to the following representation of the truncated collision operator:

$$(1.19) \quad \mathcal{Q}^R[f, f](v) = \sum_{l, m \in \mathbb{Z}^d} \left(\hat{B}(l, m) - \hat{B}(m, m) \right) \hat{f}_l \hat{f}_m E_{l+m}(v), \quad v \in \mathcal{D}_T,$$

where

$$(1.20) \quad \hat{B}(l, m) := \int_{B_R} \int_{B_R} \tilde{\mathcal{B}}(y, z) \delta(y \cdot z) E_l(y) E_m(z) dy dz, \quad l, m \in \mathbb{Z}^d.$$

It is easy to check that the coefficients $\hat{B}(l, m)$ are real and satisfy the symmetry relations

$$(1.21) \quad \hat{B}(l, m) = \hat{B}(m, l) = \hat{B}(l, -m).$$

In terms of the Fourier expansion,

$$(1.22) \quad \hat{\mathcal{Q}}^R[f, f]_k = \sum_{l, m \in \mathbb{Z}^d} \mathbf{1}(l+m-k) \left(\hat{B}(l, m) - \hat{B}(m, m) \right) \hat{f}_l \hat{f}_m, \quad k \in \mathbb{Z}^d.$$

Here $\mathbf{1}(\cdot)$ is the indicator function, equal to 1 at the origin and 0 otherwise.

The Fourier Galerkin method (FGM) in the literature (e.g. [24]) starts with a finite square grid of Fourier modes

$$(1.23) \quad K := \{k | k = (k_1, \dots, k_d), -n \leq k_1, \dots, k_d \leq n\},$$

and the subspace

$$(1.24) \quad \mathbb{P}_N = \text{span} \{E_k(v) | k \in K\} \subset L^2_{\text{per}}(\mathcal{D}_T).$$

We shall denote the grid points in K with lower-case letters j, k, l, m . FGM approximates the collision term (1.22) by projecting it to the subspace \mathbb{P}_N

$$(1.25) \quad \hat{Q}_k^{\mathcal{G}} := \sum_{l, m \in K} \mathbf{1}(l + m - k) \left(\hat{B}(l, m) - \hat{B}(m, m) \right) \hat{F}_l \hat{F}_m, \quad k \in K,$$

where \hat{F}_k for $k \in K$ serve as the approximation of the Fourier modes \hat{f}_k of the exact solution.

Putting together the above discussion, one arrives at the equations of the discrete Fourier coefficients $\hat{F}_k(t)$ for $k \in K$ for FGM [24]

$$(1.26) \quad \begin{cases} \frac{d\hat{F}_k}{dt} = \hat{Q}_k^{\mathcal{G}} = \sum_{l, m \in K} \mathbf{1}(l + m - k) \left(\hat{B}(l, m) - \hat{B}(m, m) \right) \hat{F}_l \hat{F}_m, \\ \hat{F}_k(t = 0) = \hat{F}_k^0, \end{cases}$$

where \hat{F}_k^0 are the Fourier coefficients of the initial condition $f^0(v)$ restricted on \mathcal{D}_T .

Remark 1.1. The above description of the Fourier Galerkin method is based on the Carleman representation of the Boltzmann collision operator (1.7). Starting from the classical form (1.2), one can also derive a relation similar to (1.25) (see [24] for details), while the definition of $\hat{B}(l, m)$ is slightly different:

$$(1.27) \quad \hat{B}(l, m) = \int_{B_R} \int_{\mathbb{S}^{d-1}} \mathcal{B}(g, \omega) E_l \left(\frac{1}{2}(g + |g|\omega) \right) E_m \left(\frac{1}{2}(g - |g|\omega) \right) dg d\omega,$$

where $T \geq \frac{3+\sqrt{2}}{4}R$ in the definition of $E_k(\cdot)$. It is straightforward to check that these coefficients also satisfy the symmetry relation (1.21).

FGM achieves spectral accuracy, although the computational cost is still as high as $O(N^{2d})$ [24]. Two fast algorithms [19, 11] reduced the cost to $O(MN^d \log(N))$ for the hard sphere molecules (the Maxwell molecules for 2D case) [19] and to $O(MN^{d+1} \log(N))$ for general collision kernels [11], where M is the number of points used for discretizing the unit sphere \mathbb{S}^{d-1} .

Compared to DVM, the solution of FGM loses most of the aforementioned physical properties, including positivity, the conservation of momentum and energy, and the H-theorem. In [25], Pareschi and Russo proposed a positivity preserving regularization of FGM by using Fejér filter at the expense of spectral accuracy. Despite this, the solution fails to satisfy the H-theorem. The loss of the conservation can be fixed by a spectral-Lagrangian strategy [12].

1.3. Motivation. DVM preserves a number of physical properties (such as positivity of the solution, the H-theorem, and exact conservation of mass, momentum and energy) but suffers from high computational costs and low accuracies. FGM enjoys spectral accuracies and lower computational costs but sacrifices almost all physical properties except the mass conservation. In this paper, we aim for a trade-off between the physical properties and the spectral accuracy.

As a fundamental property of the solution to the Boltzmann equation, the positivity of the distribution function helps establish the H-theorem, which is one of the crucial properties in order to guarantee the well-posedness of the discrete system. Therefore, it makes sense to maintain the positivity and the H-theorem, as long as it does not sacrifice significantly other properties such as numerical accuracy and efficiency. This paper is an initial study in this direction.

To achieve this goal, we first study carefully the reason behind the loss of the H-theorem in FGM by comparing it with DVM. With a few novel modifications to FGM, we propose an entropic Fourier method (EFM) that preserves the positivity, the mass conservation, and the H-theorem. In addition, the computational cost of this new method is the same as the one of FGM.

The rest of the paper is organized as follows. In Section 2, we first outline the key steps to develop EFM and state the main results of the paper. The details of the derivation and some deeper understandings of the model are provided in Section 3. Section 4 presents the implementation of EFM and the numerical results. The paper ends with a discussion in Section 5.

2. Main result. This section outlines the overall procedure of our derivation and lists some key results. Detailed derivation and investigation will be given in Section 3.

Aiming at developing an entropic Fourier method for the homogeneous Boltzmann equation, one works mainly with the evolution of the Fourier coefficients $\hat{F}_k(t)$. Recall the discrete Fourier transform

$$(2.1) \quad F_p = \sum_{k \in K} \hat{F}_k E_k(p), \quad \hat{F}_k = \frac{1}{N^d} \sum_{p \in X} F_p E_{-k}(p),$$

where X defined in (1.10) and K defined in (1.23) are the sets of uniform samples in the velocity space and the Fourier domain, respectively.

Using the discrete Fourier transform, one can instead treat the point values F_p as the degrees of freedom and write the numerical scheme in the DVM form (1.11). According to the derivation in Section 1.1, the following condition is required in order to guarantee the H-theorem for DVM:

CONDITION 1. *The DVM defined in (1.11) satisfies*

1. *the coefficients A_{pq}^{rs} satisfy the symmetry relation $A_{pq}^{rs} = A_{qp}^{rs} = A_{rs}^{pq}$;*
2. *the coefficients A_{pq}^{rs} are non-negative, i.e. $A_{pq}^{rs} \geq 0$;*
3. *the initial values are non-negative, i.e. $F_p(t=0) \geq 0$ for any $p \in X$.*

The general idea of our approach is to revise the existing Fourier Galerkin method (FGM) so that Condition 1 is fulfilled. Below we list the steps that lead to a numerical scheme that satisfies the H-theorem.

1. Apply the Fourier collocation method to (1.19). This leads to an approximation to (1.22) in the form

$$(2.2) \quad \hat{Q}_k^c = \sum_{l, m \in K} \mathbf{1}_N(l+m-k) [\hat{B}_N(l, m) - \hat{B}_N(m, m)] \hat{F}_l \hat{F}_m, \quad k \in K,$$

where $\mathbf{1}_N(l) := \mathbf{1}(l \bmod N)$ and $\hat{B}_N(l, m) := \hat{B}(l \bmod N, m \bmod N)$. Here \bmod is the symmetric modulo function, i.e. each component of $l \bmod N$ ranging from $-n$ to n (recall $N = 2n + 1$). Using the relation between the Fourier coefficients and the values on collocation points (2.1), we can rewrite (2.2) as

$$(2.3) \quad Q_r^C = \sum_{p, q, s \in X} A_{pq}^{rs} [F_p F_q - F_r F_s], \quad r \in X,$$

where A_{pq}^{rs} (given in (3.8)) is determined by the Fourier modes of the collision kernel $\hat{B}_N(\cdot, \cdot)$ and satisfies the symmetry relation (Condition 1.1).

2. A careful study shows that A_{pq}^{rs} fails to be non-negative. This can be fixed by applying a positivity preserving filter to $\hat{B}_N(l, m)$, i.e.,

$$(2.4) \quad \hat{B}_N^\sigma(l, m) := \hat{B}_N(l, m) \sigma_N(l) \sigma_N(m), \quad l, m \in K,$$

where $\sigma_N(l)$ is the tensor-product of d one-dimensional modified Jackson filter [17, 30]. The modified collision term takes the following form in the Fourier domain

$$\hat{Q}_k^\sigma = \sum_{l, m \in K} \mathbf{1}_N(l + m - k) [\hat{B}_N^\sigma(l, m) - \hat{B}_N^\sigma(m, m)] \hat{F}_l \hat{F}_m, \quad k \in K.$$

Using $(A^\sigma)_{pq}^{rs}$ to denote the coefficients determined by the new kernel modes $\hat{B}_N^\sigma(l, m)$ and writing

$$Q_r^\sigma = \sum_{p, q, s \in X} (A^\sigma)_{pq}^{rs} [F_p F_q - F_r F_s], \quad r \in X,$$

one can verify that both the symmetry relation (Condition 1.1) and the non-negativity (Condition 1.2) are satisfied.

3. To guarantee the positivity of the initial values (Condition 1.3), we adopt interpolation rather than orthogonal projection while discretizing the initial distribution function.

Main result. Summarizing the outline given above, we arrive at a new entropic Fourier method (EFM) that takes the following simple form

$$(2.5) \quad \begin{cases} \frac{d\hat{F}_k}{dt} = \hat{Q}_k^\sigma = \sum_{l, m \in K} \mathbf{1}_N(l + m - k) \left(\hat{B}_N^\sigma(l, m) - \hat{B}_N^\sigma(m, m) \right) \hat{F}_l \hat{F}_m, \\ \hat{F}_k(t = 0) = \frac{1}{N^d} \sum_{r \in X} f(t = 0, r) E_{-k}(r). \end{cases}$$

This method preserves several key physical properties, as guaranteed by the following theorem.

THEOREM 2.1. *If $f(t = 0, v) \geq 0$ for $v \in \mathbb{R}^d$, then the solution $F_r(t) = \sum_{k \in K} \hat{F}_k(t) E_k(r)$ for $r \in X$ of (2.5) satisfies for $\forall t > 0$,*

$$(2.6) \quad \text{conservation of mass: } \frac{d}{dt} \sum_{r \in X} F_r(t) = 0,$$

$$(2.7) \quad \text{non-negativity: } F_r(t) \geq 0, \quad r \in X,$$

$$(2.8) \quad \text{discrete H-theorem: } \frac{d}{dt} \sum_{r \in X} F_r(t) \ln F_r(t) \leq 0.$$

The proof is presented in Section 3.5. Due to the positivity-preserving filter (3.21), the numerical accuracy of EFM in approximating the collision operator is second order (see Section 3.4 for details).

Another important result for EFM is the existence of fast algorithms. For FGM, the fast algorithms proposed in [19, 11] are based on the approximation of the kernel $\hat{B}_N(\cdot, \cdot)$:

$$(2.9) \quad \hat{B}_N(l, m) \approx \sum_{t=1}^M \alpha_{l+m}^t \beta_l^t \gamma_m^t, \quad l, m \in K,$$

with the number of terms $M \ll N^d$. Since the filtered kernel $\hat{B}_N^\sigma(l, m)$ turns out to have a similar approximation

$$(2.10) \quad \hat{B}_N^\sigma(l, m) \approx \sum_{t=1}^M \alpha_{l+m}^t (\sigma_N(l) \beta_l^t) (\sigma_N(m) \gamma_m^t),$$

these fast algorithms still apply. Moreover, when the above approximation is applied, the H-theorem still holds. Detailed discussion will be given in Section 4.1.

3. Entropic Fourier method. As shown in Section 1.1, a discrete H-theorem can be obtained from the classical DVM, where the associated entropy function can be considered as a numerical quadrature for the integral of $f \ln f$. This requires the positivity of the distribution function, which can be guaranteed by the positivity of the discrete collision kernel A_{pq}^{rs} . In general, to preserve the Boltzmann entropy in the numerical scheme, the positivity of the numerical solution needs to be enforced in a certain sense due to the presence of $\ln f$ in the entropy function. However, in FGM, there is no guarantee of any form of positivity in the numerical solution, and hence the H-theorem does not hold.

In this paper, rather than enforcing the non-negativity of the whole distribution function, we take a collocation approach and focus on the non-negativity only at the collocation points. Based on this idea, we start from a collocation method for the homogeneous Boltzmann equation and write it as a DVM of the function values defined at the collocation points. One then tries to alter the coefficients to match the requirements in Condition 1 so that the H-theorem can be subsequently derived.

The three steps listed in Section 2 are elaborated in the first three subsections below. After that, Section 3.4 compares the entropic Fourier method (EFM) with other Fourier methods.

3.1. Fourier collocation method in a DVM form. The mechanisms of DVM and FGM are quite different: DVM is concerned with the values of the distribution on discrete points, whereas FGM (1.25), as a Galerkin method, works on the Fourier modes of the distribution function. It is not straightforward how to link these two methods. Alternatively, we will consider another type of Fourier methods — the collocation method (also known as the pseudospectral method).

3.1.1. Fourier collocation method. In the Fourier collocation method (FCM), the collision term on the set X is evaluated directly using (1.19):

$$(3.1) \quad Q_r^C = \sum_{l, m \in K} \left(\hat{B}_N(l, m) - \hat{B}_N(m, m) \right) \hat{F}_l \hat{F}_m E_{l+m}(r), \quad r \in X,$$

where $\hat{B}_N(l, m) := \hat{B}(l \bmod N, m \bmod N)$, and mod is the symmetric modulo function, i.e. each component of $l \bmod N$ ranging from $-n$ to n (recall $N = 2n + 1$). Since

the above equation only uses the value of \hat{B}_N in K , one can use \hat{B} and \hat{B}_N interchangeably here. Here we note that $\hat{B}_N(l, m)$ satisfy the symmetry relation (1.21).

The corresponding Fourier modes can be obtained by an inverse discrete Fourier transform:

$$(3.2) \quad \begin{aligned} \hat{Q}_k^C &= \frac{1}{N^d} \sum_{r \in X} Q_r E_{-k}(r) \\ &= \sum_{l, m \in K} \mathbf{1}_N(l + m - k) \left(\hat{B}_N(l, m) - \hat{B}_N(m, m) \right) \hat{F}_l \hat{F}_m, \end{aligned}$$

where $\mathbf{1}_N(l) := \mathbf{1}(l \bmod N)$.

If the initial value is smooth enough, due to the smoothing effect of the Boltzmann collision operator [1], both the Fourier Galerkin and the Fourier collocation methods have spectral accuracy [8]. Moreover, in some cases, FCM (3.2) is numerically more efficient, especially for the fast summation algorithms in [19, 11]. For example, in [19], the following approximation of $\hat{B}_N(l, m)$ is considered:

$$(3.3) \quad \hat{B}_N(l, m) \approx \sum_{t=1}^M \beta_l^t \gamma_m^t,$$

where $M \in \mathbb{N}^+$ is the total number of quadrature points on the sphere. Then the collision term in this Galerkin method can be approximated by

$$(3.4) \quad \sum_{t=1}^M \sum_{l, m \in K} \mathbf{1}(l + m - k) \left[\left(\beta_l^t \hat{F}_l \right) \left(\gamma_m^t \hat{F}_m \right) - \hat{F}_l \left(\beta_m^t \gamma_m^t \hat{F}_m \right) \right].$$

To evaluate (3.4) efficiently, one needs to utilize FFT-based convolutions. To obtain these coefficients, one needs the zero-padding technique to avoid aliasing. If one uses the same method to evaluate \hat{Q}_k in (3.2), then no zero padding is needed. Therefore the collocation method shortens the length of vectors used in the Fourier transform, which makes the algorithm faster.

3.1.2. DVM form. To link FCM with DVM, we split the collision term (3.1) into the gain part (+) and the loss part (-):

$$(3.5) \quad Q_r^{C,+} = \sum_{l, m \in K} \hat{B}_N(l, m) \hat{F}_l \hat{F}_m E_{l+m}(r), \quad Q_r^{C,-} = \sum_{l, m \in K} \hat{B}_N(m, m) \hat{F}_l \hat{F}_m E_{l+m}(r), \quad r \in X.$$

Noticing $E_{l+m}(r) = \sum_{k \in K} \mathbf{1}_N(l + m - k) E_k(r)$ and plugging (2.1) into the gain part yields

$$(3.6) \quad Q_r^{C,+} = \frac{1}{N^{2d}} \sum_{\substack{l, m, k \in K \\ p, q \in X}} \mathbf{1}_N(l + m - k) \hat{B}_N(l, m) E_{-l}(p) E_{-m}(q) E_k(r) F_p F_q.$$

Since $\frac{1}{N^d} \sum_{s \in X} E_j(s) = \mathbf{1}_N(j)$, one can sum over j to get $\frac{1}{N^d} \sum_{j \in K, s \in X} E_j(s) = 1$. With this equation, one introduces two new indices to (3.6) by multiplying its right hand side with $\frac{1}{N^d} \sum_{j \in K, s \in X} E_j(s)$:

$$(3.7) \quad Q_r^{C,+} = \frac{1}{N^{3d}} \sum_{\substack{l, m, k, j \in K \\ p, q, s \in X}} \mathbf{1}_N(l + m - k - j) \hat{B}_N(l - j, m - j) E_{-l}(p) E_{-m}(q) E_k(r) E_j(s) F_p F_q.$$

If one introduces

$$(3.8) \quad A_{pq}^{rs} = \frac{1}{N^{3d}} \sum_{l,m,k,j \in K} \mathbf{1}_N(l+m-k-j) \hat{B}_N(l-j, m-j) E_{-l}(p) E_{-m}(q) E_k(r) E_j(s),$$

then the gain term is

$$(3.9) \quad Q_r^{\mathcal{C},+} = \sum_{p,q,s \in X} A_{pq}^{rs} F_p F_q.$$

Apparently, such term does take the form of the gain term of DVM (1.11).

For the loss term, the identity

$$(3.10) \quad \sum_{p,q \in X} A_{pq}^{rs} = \frac{1}{N^d} \sum_{k,j} \mathbf{1}_N(k+j) \hat{B}_N(j,j) E_k(r) E_j(s),$$

leads to the following derivation

$$(3.11) \quad \begin{aligned} \sum_{p,q,s \in X} A_{pq}^{rs} F_r F_s &= \frac{1}{N^d} \sum_{k,j \in K, s \in X} \mathbf{1}_N(k+j) \hat{B}_N(j,j) E_k(r) E_j(s) F_r F_s \\ &= \frac{1}{N^d} \sum_{k,j,l,m \in K, s \in X} \mathbf{1}_N(k+j) \hat{B}_N(j,j) E_k(r) E_j(s) E_l(r) E_m(s) \hat{F}_l \hat{F}_m \\ &= \sum_{k,j,l,m \in K} \mathbf{1}_N(k+j) \mathbf{1}_N(j+m) \hat{B}_N(j,j) \hat{F}_l \hat{F}_m E_{k+l}(r) \\ &= \sum_{l,m \in K} \hat{B}_N(m,m) \hat{F}_l \hat{F}_m E_{l+m}(r) = Q_r^{\mathcal{C},-}. \end{aligned}$$

In summary, one can write FCM in the following DVM form

$$(3.12) \quad Q_r^{\mathcal{C}} = \sum_{p,q,s \in X} A_{pq}^{rs} (F_p F_q - F_r F_s)$$

with A_{pq}^{rs} given in (3.8). Finally, the symmetry relation (Condition 1.1)

$$(3.13) \quad A_{pq}^{rs} = A_{qp}^{rs} = A_{rs}^{pq}$$

holds, as this can be easily seen by the symmetry relation of $\hat{B}_N(l,m)$ and switching the indices in (3.8).

3.2. Positivity preserving. As remarked earlier, in order to obtain an H-theorem for FCM, one needs to ensure that all the coefficients A_{pq}^{rs} are non-negative (Condition 1.2). Below, we first show that A_{pq}^{rs} as defined in (3.12) fail to be non-negative, and then apply a filter to recover non-negativity.

3.2.1. Failure of positivity preservation in FCM. We start by simplifying the coefficients A_{pq}^{rs} based on (3.8)

$$(3.14) \quad \begin{aligned} A_{pq}^{rs} &= \frac{1}{N^{3d}} \sum_{l,m,k,j \in K} \mathbf{1}_N(l+m-k-j) \hat{B}_N(l-j, m-j) E_{-l}(p) E_{-m}(q) E_k(r) E_j(s) \\ &= \frac{1}{N^{3d}} \sum_{l,m,k \in K} \hat{B}_N(m-k, l-k) E_{-l}(p-s) E_{-m}(q-s) E_k(r-s). \end{aligned}$$

where one uses $j = l + m - k \bmod N$. By performing a change of variables $i = (m - k) \bmod N$ and $j = (l - k) \bmod N$, we arrive at

$$(3.15) \quad \begin{aligned} A_{pq}^{rs} &= \frac{1}{N^{3d}} \sum_{i,j,k \in K} \hat{B}_N(i,j) E_{-k-i}(p-s) E_{-k-j}(q-s) E_k(r-s) \\ &= \mathbf{1}_N(r+s-p-q) \frac{1}{N^{2d}} \sum_{i,j \in K} \hat{B}_N(i,j) E_{-i}(p-s) E_{-j}(q-s). \end{aligned}$$

By introducing

$$(3.16) \quad G(y, z) = \sum_{i,j \in K} \hat{B}_N(i,j) E_{-i}(y) E_{-j}(z), \quad y, z \in \mathcal{D}_T,$$

which is by definition a periodic function with period \mathcal{D}_T , one can write compactly

$$(3.17) \quad A_{pq}^{rs} = \frac{1}{N^{2d}} \mathbf{1}_N(r+s-p-q) G(p-s, q-s), \quad p, q, r, s \in X.$$

In order to check whether A_{pq}^{rs} is non-negative, one just needs to check whether $G(\cdot, \cdot)$ is non-negative on the collocation points in X . To get a better understanding of the function $G(\cdot, \cdot)$ as defined in (3.16), one applies the definition of $\hat{B}_N(\cdot, \cdot)$ to obtain

$$(3.18) \quad G(y, z) = \int_{B_R} \int_{B_R} \tilde{\mathcal{B}}(y', z') \delta(y' \cdot z') \chi_N(y - y') \chi_N(z - z') dy' dz'.$$

Here χ_N is the Dirichlet kernel over \mathcal{D}_T defined by

$$(3.19) \quad \chi_N(v) = \sum_{k \in K} E_k(v), \quad v \in \mathcal{D}_T,$$

and its discrete Fourier transform $\hat{\chi}_N(k)$ is equal to 1 for $k \in K$ and 0 on $\mathbb{Z}^d \setminus K$. By introducing a periodic function in \mathcal{D}_T

$$(3.20) \quad H(y, z) = \tilde{\mathcal{B}}(y, z) \delta(y \cdot z) \mathbf{1}(|y| \leq R) \mathbf{1}(|z| \leq R), \quad y, z \in \mathcal{D}_T,$$

one can write

$$G = H * (\chi_N \otimes \chi_N),$$

where the convolution is defined periodically in $\mathcal{D}_T \times \mathcal{D}_T$. Equivalently, $G(y, z)$ is also the truncated Fourier expansion of $H(y, z)$ by keeping only the frequencies in K .

Although $H(y, z)$ is non-negative in the weak sense, its truncated Fourier approximation $G(y, z)$ fails to be so. For example, the values of G for the kernel $\tilde{\mathcal{B}}(y, z) \equiv \frac{1}{\pi}$, $R = 6$ in 2D are plotted in Figure 1. This clearly shows that negative values appear as expected. Therefore in general, the H-theorem does not hold for FCM.

3.2.2. Filtering. In the previous subsection, one can see that if $\chi_N(\cdot)$ were a non-negative function, then $G(y, z)$ would be non-negative for any y and z . Thus, in order to get non-negative coefficients, a possible way is to replace the function χ_N by a non-negative one. Note that $\chi_N(v)$ is Dirichlet kernel, which is an approximation of the Dirac delta. As $N \rightarrow +\infty$, the function $\chi_N(\cdot)$ tends to Dirac delta weakly in an oscillatory way. As pointed out in [10], the oscillation breaks the non-negativity of the solution.

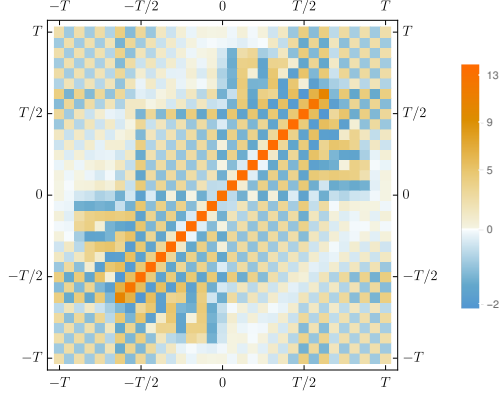


FIG. 1. The values of $G(y, z)$ with $N = 32$ at $z = (T/2, T/2)$. The axes are the two components of y .

As mentioned earlier in Section 2, we adopt the one-dimensional modified Jackson filter [17, 30] given by

$$(3.21) \quad \sigma_N(\beta) = \frac{(n+1-|\beta|)\cos(\frac{\pi|\beta|}{n+1}) + \sin(\frac{\pi|\beta|}{n+1})\cot(\frac{\pi}{n+1})}{n+1},$$

where $N = 2n + 1$ and $-n \leq \beta \leq n$. By a slight abuse of notation, the d -dimensional modified Jackson filter for a multiindex $k = (k_1, \dots, k_d) \in K$ is defined through tensor-product

$$\sigma_N(k) = \prod_{i=1}^d \sigma_N(k_i).$$

The modified kernel $\chi_N^\sigma(v)$ can then be defined as

$$\chi_N^\sigma(v) = \sum_{k \in K} \sigma_N(k) E_k(v), \quad v \in \mathcal{D}_T.$$

Once χ_N is replaced with χ_N^σ in (3.18), the function $G(y, z)$ is substituted with $G^\sigma(y, z) := (G * (\chi_N^\sigma \otimes \chi_N^\sigma))(y, z)$. A direct calculation shows that

$$(3.22) \quad \begin{aligned} G^\sigma(y, z) &= \frac{1}{N^{2d}} \int_{B_R} \int_{B_R} \tilde{\mathcal{B}}(y', z') \delta(y' \cdot z') \chi_N^\sigma(y - y') \chi_N^\sigma(z - z') dy' dz' \\ &= \frac{1}{N^{2d}} \sum_{l, m \in K} \int_{B_R} \int_{B_R} \tilde{\mathcal{B}}(y', z') \delta(y' \cdot z') \sigma_N(l) \sigma_N(m) E_l(y - y') E_m(z - z') dy' dz' \\ &= \frac{1}{N^{2d}} \sum_{l, m \in K} [\sigma_N(l) \sigma_N(m) \hat{B}_N(l, m)] E_{-l}(y) E_{-m}(z) \\ &= \frac{1}{N^{2d}} \sum_{l, m \in K} \hat{B}_N^\sigma(l, m) E_{-l}(y) E_{-m}(z), \end{aligned}$$

where $\hat{B}_N^\sigma(l, m) := \hat{B}_N(l, m) \sigma_N(l) \sigma_N(m)$ as defined in (2.4). With $G^\sigma(y, z) \geq 0$ guaranteed, one can mimic (3.17) and define

$$(3.23) \quad (A^\sigma)_{pq}^{rs} = \frac{1}{N^{2d}} \mathbf{1}_N(r + s - p - q) G^\sigma(p - s, q - s), \quad p, q, r, s \in X,$$

which are apparently non-negative. Since replacing $\hat{B}_N(l, m)$ with $\hat{B}_N^\sigma(l, m)$ does not affect the symmetry relation (1.21), the new coefficients $(A^\sigma)_{pq}^{rs}$ also satisfies $(A^\sigma)_{pq}^{rs} = (A^\sigma)_{qp}^{rs} = (A^\sigma)_{rs}^{pq}$.

From the above discussion, we now define the entropic collision term to be

$$(3.24) \quad \hat{Q}_k^\sigma := \sum_{l, m \in K} \mathbf{1}_N(l + m - k) \left(\hat{B}_N^\sigma(l, m) - \hat{B}_N^\sigma(m, m) \right) \hat{F}_l \hat{F}_m, \quad k \in K$$

in the Fourier domain. In the velocity domain, it is equal to

$$(3.25) \quad Q_r^\sigma := \sum_{p, q, s \in X} (A^\sigma)_{pq}^{rs} (F_p F_q - F_r F_s), \quad r \in X.$$

3.3. Initial condition. In order to obtain the H-theorem, one needs to make sure that the initial data are non-negative. Since the collision term in (3.25) depends only on the values at the collocation points in X , it is sufficient to make the initial data non-negative at these collocation points. Consequently, it is natural to use sampling rather than orthogonal projection while preparing the discrete initial data F_r^0 for $r \in X$. More precisely,

$$(3.26) \quad F_r^0 = \mathcal{I}_N f^0 := \begin{cases} f^0(r), & f^0 \text{ is continuous,} \\ (\varphi^\epsilon * f^0)(r), & \text{otherwise,} \end{cases}$$

where $\varphi^\epsilon \geq 0$ is a mollifier, such that $\|f^0 - \varphi^\epsilon * f^0\|_{L^2} < \epsilon$ for ϵ sufficiently small. Once $\{F_r^0\}$ are ready, the corresponding Fourier coefficients $\{\hat{F}_k^0\}$ are computed via a fast Fourier transform.

At this point, all ingredients of the entropic Fourier method (EFM) are ready. The Cauchy problem of EFM takes the following form as a DVM

$$(3.27) \quad \begin{cases} \frac{dF_r}{dt} = Q_r^\sigma = \sum_{p, q, s \in X} (A^\sigma)_{pq}^{rs} (F_p F_q - F_r F_s), \\ F_r(t=0) = F_r^0, \end{cases}$$

Equivalently in the Fourier domain, EFM takes the form

$$(3.28) \quad \begin{cases} \frac{d\hat{F}_k}{dt} = \hat{Q}_k^\sigma = \sum_{l, m \in K} \mathbf{1}_N(l + m - k) \left(\hat{B}_N^\sigma(l, m) - \hat{B}_N^\sigma(m, m) \right) \hat{F}_l \hat{F}_m, \\ \hat{F}_k(t=0) = \hat{F}_k^0. \end{cases}$$

Remark 3.1. The same technique can be applied to the Fourier method derived from the classical form of the Boltzmann collision operator (1.2) to obtain an entropic Fourier method. In fact, from (1.27) and following the definition of $G(y, z)$ in (3.16), one can directly obtain

$$G(y, z) = (H * (\chi_N \otimes \chi_N))(y, z), \quad H(g, g') = \mathcal{B}(g, \omega) \delta(|g| - |g'|) \mathbf{1}(|g| \leq R), \quad g, g' \in \mathcal{D}_T.$$

Again, by (3.17), the positivity of A_{pq}^{rs} depends only on the positivity of $G(y, z)$ at the collocation points. Therefore, replacing χ_N with χ_N^σ does the job.

3.4. Comparison. The derivation of EFM switched frequently between the language of Fourier methods and DVM for different purposes. As we have shown in (3.27) and (3.28), EFM can be regarded either as a Fourier method or as a special DVM.

In what follows, we provide a comparison between the entropic Fourier method (EFM), the FGM (Fourier Galerkin method), and the Fourier collocation method (FCM). To set up a uniform notation, let $\mathcal{Q}[\cdot; \cdot, \cdot]$ be the general collision operator

$$(3.29) \quad \mathcal{Q}[C; f, f](v) = \int_{\mathcal{D}_T} \int_{\mathcal{D}_T} C(y, z) [f(v+y)f(v+z) - f(v)f(v+y+z)] dy dz$$

with a collision kernel $C(\cdot, \cdot)$. Thus the truncated collision term (1.17) can be written as $\mathcal{Q}(H; f, f)$ using the definition of H in (3.20).

Notice that a special feature of a function in \mathbb{P}_N is that it is uniquely defined via its function values at points in X defined in (1.10). Therefore, $\{F_p | p \in X\}$ can be regarded both as discrete set of values or the samples from the smooth periodic $F(v) \in \mathbb{P}_N \subset L^2_{\text{per}}(\mathcal{D}_T)$. By introducing two operators

$$\mathcal{P}_N : f \rightarrow \chi_N * f, \quad \mathcal{S}_N^\sigma : f \rightarrow \chi_N^\sigma * f$$

for the space $L^2_{\text{per}}(\mathcal{D}_T)$, the three methods are different approximations of $\mathcal{Q}(H; f, f)$ with different initial values:

$$(3.30) \quad \text{FGM: } \mathcal{P}_N \mathcal{Q}[(\mathcal{P}_N \otimes \mathcal{P}_N)H; F, F], \quad F(t=0, v) = \mathcal{P}_N f(t=0, v),$$

$$(3.31) \quad \text{FCM: } \underline{\mathcal{I}}_N \mathcal{Q}[(\mathcal{P}_N \otimes \mathcal{P}_N)H; F, F], \quad F(t=0, v) = \mathcal{P}_N f(t=0, v),$$

$$(3.32) \quad \text{EFM: } \underline{\mathcal{I}}_N \mathcal{Q}[(\mathcal{S}_N^\sigma \otimes \mathcal{S}_N^\sigma)H; F, F], \quad F(t=0, v) = \underline{\mathcal{I}}_N f(t=0, v).$$

where $\underline{\mathcal{I}}_N$ is the interpolation operator defined in (3.26).

The list (3.30) to (3.32) clearly shows how we change from FGM to EFM in our derivation. The last line (3.32) also shows that EFM provides an approximation of the original binary collision operator in the language of spectral methods. Below we will briefly review the basic properties of all the three methods.

The method (3.30) stands for FGM as described in Section 1.2. In the derivation, the kernel K is not explicitly projected. However, (1.25) shows that the discrete collision operator depends only on $(\mathcal{P}_N \times \mathcal{P}_N)H$. By replacing the projection operator applied to \mathcal{Q} with interpolation as in (3.2), we arrive at the Fourier collocation method (3.31) introduced in Section 3.1. Since a direct projection of H does not preserve the positivity of the kernel, the negative part of the discrete kernel may cause a violation of the H-theorem. Nevertheless, both these two methods have spectral accuracy in the velocity space.

To ensure the positivity of the discrete kernel, the filter $\mathcal{S}_N^\sigma \otimes \mathcal{S}_N^\sigma$ is applied in (3.32), and thus positive coefficients (3.23) are obtained. The method (3.32) also ensures the positivity of the approximation of F at collocation points, and thus the discrete H-theorem follows.

However, the filter \mathcal{S}_N^σ has a smearing effect, which reduces the order of convergence. For any smooth periodic function $f \in L^2_{\text{per}}(\mathcal{D}_T)$, the L^2 -error $\|f - \mathcal{S}_N^\sigma f\|_2$ is $O(N^{-2})$ [16, Chapter 4], and therefore EFM is at most second-order. On the other hand, if one splits the collision term of EFM into the gain part and the loss part and

let $F = \mathcal{P}_N f$, then

(3.33)

$$Q^{\sigma,+}[F, F](r) = \sum_{l,m \in K} \hat{B}_N(l, m) \sigma_N(l) \hat{F}_l \sigma_N(m) \hat{F}_m E_{l+m}(r) = Q^{\mathcal{C},+}[\mathcal{S}_N^\sigma F, \mathcal{S}_N^\sigma F](r),$$

(3.34)

$$Q^{\sigma,-}[F, F](r) = \sum_{l,m \in K} \hat{B}_N(m, m) \hat{F}_l \sigma_N^2(m) \hat{F}_m E_{l+m}(r) = Q^{\mathcal{C},-}[F, \mathcal{S}_N^\sigma \mathcal{S}_N^\sigma F](r),$$

for any $r \in X$. Following the boundedness of the truncated collision operator proven in [24], one concludes that

$$\|Q^\sigma[F, F] - Q^{\mathcal{C}}[F, F]\|_2 \leq \|Q^{\sigma,+}[F, F] - Q^{\mathcal{C},+}[F, F]\|_2 + \|Q^{\sigma,-}[F, F] - Q^{\mathcal{C},-}[F, F]\|_2 \leq O(N^{-2}).$$

Hence, EFM has second-order accuracy in approximating the truncated collision operator, if the distribution is smooth enough (due to the smoothing effect of the Boltzmann collision operator [1], we only the initial value is smooth enough). This order of convergence will be also numerically verified in the next section.

3.5. Proof of Theorem 2.1. This subsection provides the proof of Theorem 2.1.

Proof of Theorem 2.1. The argument in Section 3.2.2 indicates that if $f(t = 0, v) \geq 0$, then the coefficients A_{pq}^{rs} and the initial values F_r^0 satisfy all the three conditions in Condition 1.

The symmetry relation (1.21) of $\hat{B}(l, m)$ and the definition of $\hat{B}_N^\sigma(l, m)$ indicates $\mathbf{1}_N(l+m) \left(\hat{B}_N^\sigma(l, m) - \hat{B}_N^\sigma(m, m) \right) = 0$, i.e. $Q_0^\sigma = 0$. Noticing that the zero frequency $\hat{F}_0(t) = \frac{1}{N^d} \sum_{r \in X} F_r(t)$, one can directly obtain the conservation of mass (2.6).

Since $f^0(v) \geq 0$, $F_r^0 \geq 0$ by construction. If there exists $t' > 0$ and $r \in X$ such that $F_r(t') = 0$ and $F_p(t') \geq 0$ for any other $p \in X$, then

$$\left. \frac{dF_r(t)}{dt} \right|_{t=t'} = \sum_{p,q,s \in X} (A^\sigma)_{pq}^{rs} F_p F_q \geq 0,$$

which indicates $F_r(t) \geq 0$ for all $t > 0$ and $r \in X$.

The symmetry relation and non-negativity of $(A^\sigma)_{pq}^{rs}$ indicate the discrete H-theorem (2.8)

$$\sum_{r \in X} Q_r^\sigma \ln(F_r) = \frac{1}{4} \sum_{p,q,r,s \in X} (A^\sigma)_{pq}^{rs} \ln \left(\frac{F_r F_s}{F_p F_q} \right) [F_p F_q - F_r F_s] \leq 0.$$

This completes the proof. \square

4. Numerical tests. This section describes several numerical tests to demonstrate the properties of EFM and to compare with the Fourier Galerkin method (FGM) in [24] and the positivity preserving spectral method (PPSM) in [25].

4.1. Implementation. It is pointed out in Section 2 that the fast algorithms in [19, 11] can be applied to EFM without affecting the H-theorem. To show this, one needs to check that the fast algorithms do not violate the first two conditions in Condition 1.

These fast algorithms are based on an approximation of $\hat{B}_N(l, m)$ (2.10) of the following form.

$$(4.1) \quad \hat{B}_N(l, m) \approx \hat{B}_{N,\text{fast}}(l, m) := \sum_{t=1}^M \alpha_{l+m}^t \beta_l^t \gamma_m^t.$$

After the filtering is applied, one obtains a similar approximation for $\hat{B}_N^\sigma(l, m)$

$$(4.2) \quad \hat{B}_N^\sigma(l, m) \approx \hat{B}_{N,\text{fast}}^\sigma(l, m) := \sum_{t=1}^M \alpha_{l+m}^t (\sigma_N(l) \beta_l^t) (\sigma_N(m) \gamma_m^t).$$

It can be verified that both kernels satisfy the symmetry relation

$$(4.3) \quad \hat{B}_{N,\text{fast}}(l, m) = \hat{B}_{N,\text{fast}}(m, l) = \hat{B}_{N,\text{fast}}(-l, m),$$

$$(4.4) \quad \hat{B}_{N,\text{fast}}^\sigma(l, m) = \hat{B}_{N,\text{fast}}^\sigma(m, l) = \hat{B}_{N,\text{fast}}^\sigma(-l, m),$$

which indicates Condition 1.1 is valid for the fast algorithms.

To see that the fast algorithms do not affect the non-negativity of $G^\sigma(y, z)$, we use the fast algorithm in [19] with $d = 2$ and $\bar{B} = 1$ as an example. The first step of this algorithm writes y and z in (1.20) in the polar coordinates $y = \rho e$ and $z = \rho_* e_*$:

$$(4.5) \quad \hat{B}_N(l, m) = \frac{1}{4} \int_{\mathbb{S}^1} \int_{\mathbb{S}^1} \delta(e \cdot e_*) \left[\int_{-R}^R E_l(\rho e) d\rho \right] \left[\int_{-R}^R E_m(\rho_* e_*) d\rho_* \right] de de_*.$$

Let $\psi_R(l, e) = \int_{-R}^R E_l(\rho e) d\rho$, then

$$\hat{B}_N(l, m) = \frac{1}{4} \int_{\mathbb{S}^1} \int_{\mathbb{S}^1} \delta(e \cdot e_*) \psi_R(l, e) \psi_R(m, e_*) de de_*.$$

Integrating it with respect to e_* yields

$$(4.6) \quad \hat{B}_N(l, m) = \int_0^\pi \psi_R(l, e_\theta) \psi_R(m, e_{\theta+\pi/2}) d\theta.$$

Substituting (4.5) into (3.22) gives rise to

$$(4.7) \quad G^\sigma(y, z) = \frac{1}{4} \int_{\mathbb{S}^1} \int_{\mathbb{S}^1} \delta(e \cdot e_*) \left[\int_{-R}^R \chi_N^\sigma(\rho e - y) d\rho \right] \left[\int_{-R}^R \chi_N^\sigma(\rho_* e_* - z) d\rho_* \right] de de_*.$$

Let $\phi_R^\sigma(y, e) = \int_{-R}^R \chi_N^\sigma(\rho e - y) d\rho$. Apparently, $\phi_R^\sigma(y, e) \geq 0$ due to $\chi_N^\sigma(y) \geq 0$ for any $y \in \mathbb{R}^2$. Then integrating (4.7) with respect to e_* yields

$$(4.8) \quad G^\sigma(y, z) = \int_0^\pi \phi_R^\sigma(y, e_\theta) \phi_R^\sigma(z, e_{\theta+\pi/2}) d\theta.$$

The idea of the fast algorithm is to replace the integration in (4.6) with a quadrature formula. More precisely (4.6) is approximated by

$$(4.9) \quad \hat{B}_{N,\text{fast}}(l, m) = \sum_{t=1}^M \frac{\pi}{M} \psi_R(l, e_{\theta_t}) \psi_R(m, e_{\theta_t+\pi/2}).$$

Similarly to (4.9), one obtains

$$(4.10) \quad G_{\text{fast}}^\sigma(y, z) = \sum_{t=1}^M \frac{\pi}{M} \phi_R^\sigma(y, e_{\theta_t}) \phi_R^\sigma(z, e_{\theta_t + \pi/2}).$$

Since $\phi_R^\sigma(y, e) \geq 0$ for any $y \in \mathbb{R}^2$, $e \in \mathbb{S}^1$, $G_{\text{fast}}^\sigma(y, z) \geq 0$ for any $y, z \in \mathbb{R}^2$. Hence, the fast algorithm does not destroy the non-negativity of $G_{\text{fast}}^\sigma(y, z)$.

As we pointed out in Section 3.1, an aliased convolution can be directly used to calculate (2.5). Since the accuracy of EFM is only second order, the smoothing filter is the main source of the error. In the fast algorithms, the number M in (4.1) perhaps can be smaller than that in [19, 11].

In the above discussion, we only study the case when N is odd. The case of even N values can be reduced to the odd $(N - 1)$ case by setting the coefficient of a mode k to be zero 0 if any component of $k = (k_1, \dots, k_d)$ is equal to $-N/2$.

For the time discretization, the third-order strong stability-preserving Runge-Kutta method proposed in [14] is employed in the discretization of time. In all tests, the time step is chosen as $\Delta t = 0.01$.

4.2. Numerical results. The test problems used here are solutions of the space-homogeneous Boltzmann equation for Maxwell molecules ($\mathcal{B}(g, \omega) = \frac{1}{2\pi}$ in 2D and $\mathcal{B}(g, \omega) = \frac{1}{4\pi}$ in 3D).

Example 1 (2D BKW solution). The first example is the well-known 2D BKW solution, obtained independently in [3] and [15]. The exact solution takes the form

$$(4.11) \quad f(t, v) = \frac{1}{2\pi S} \exp\left(-\frac{|v|^2}{2S}\right) \left(\frac{2S-1}{S} + \frac{1-S}{2S^2}|v|^2\right),$$

where $S = 1 - \exp(-t/8)/2$. The BKW solution allows one to check the accuracy, positivity of the solution, and the entropy of the proposed method. Here we set the truncation radius $R = 6$ in the tests.

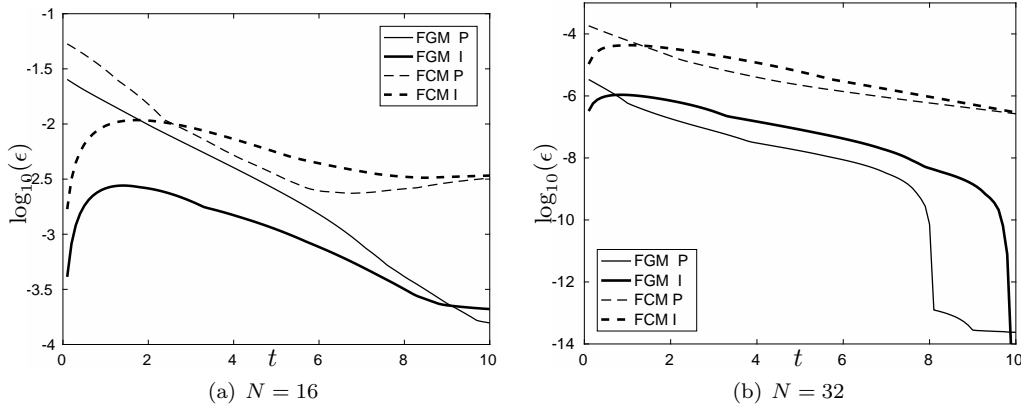


FIG. 2. Positivity error of FGM and FCM with the initial value prepared by orthogonal projection (P) and interpolation (I) in the \log_{10} scale. Since the positivity error of EFM is strictly zero, its result is not plotted in the figure.

Both FGM (1.26) or FCM (3.2) result in good approximations of the exact solution at the collocation points. However, the solutions are not non-negative. Even if we

use interpolation rather than orthogonal projection to prepare the initial values, the solutions of these methods still fail to be non-negative. The positivity of the solution is measured by the positivity error defined via

$$(4.12) \quad \epsilon := \frac{\sum_{q \in X} |F_q| - \sum_{q \in X} F_q}{\sum_{q \in X} |F_q|}.$$

Figure 2 shows that both FGM and FCM fail to preserve the positivity of the solution at the collocation points no matter whether the initial value is given by orthogonal projection or interpolation. On the other hand, the positivity error of EFM is strictly zero, thanks to the modification in (3.22).

Table 1 summarizes the ℓ_1 , ℓ_2 and ℓ_∞ errors of (3.27) at time $t = 0.01$. Here the ℓ_p relative errors for $p = 1, 2, \infty$ are defined by

$$(4.13) \quad \frac{\|F - f\|_p}{\|f\|_p} = \frac{\left(\sum_{q \in X} |F_q - f(q)|^p\right)^{1/p}}{\left(\sum_{q \in X} |f(q)|^p\right)^{1/p}},$$

where $f(q)$ is the exact solution at $q \in X$. The numerical results also show that the convergence rate of EFM is of second order.

N	ℓ_1 error	rate	ℓ_2 error	rate	ℓ_∞ error	rate
16	4.68×10^{-3}		3.23×10^{-3}		3.12×10^{-3}	
32	1.72×10^{-3}	1.44	1.36×10^{-3}	1.25	1.40×10^{-3}	1.15
64	5.54×10^{-4}	1.64	4.56×10^{-4}	1.58	5.57×10^{-4}	1.34
128	1.55×10^{-4}	1.84	1.29×10^{-4}	1.82	1.73×10^{-4}	1.68
256	4.05×10^{-5}	1.93	3.42×10^{-5}	1.92	4.73×10^{-5}	1.87
512	1.03×10^{-5}	1.97	8.76×10^{-6}	1.96	1.22×10^{-5}	1.94

TABLE 1

The ℓ_1 , ℓ_2 and ℓ_∞ errors and convergence rates for the BKW solution at time $t = 0.01$ with $R = 6$.

As discussed in Section 4.1, the fast algorithm in [19] can be applied to EFM to accelerate the computation. In (4.6), the integration on $[0, \pi]$ can be reduced to $[0, \pi/2]$ and M is equal to the number of samples within $[0, \pi/2]$. Table 2 presents the ℓ_1 error for multiple values of M , noticing that $M = 2$ is good enough in practice while in [19] the authors suggest $M \geq 4$.

N	$M = 2$	$M = 3$	$M = 32$
16	4.6852×10^{-3}	4.6826×10^{-3}	4.6830×10^{-3}
32	1.7241×10^{-3}	1.7244×10^{-3}	1.7245×10^{-3}
64	5.5368×10^{-4}	5.5388×10^{-4}	5.5394×10^{-4}
128	1.5485×10^{-4}	1.5488×10^{-4}	1.5489×10^{-4}
256	4.0513×10^{-5}	4.0516×10^{-5}	4.0517×10^{-5}

TABLE 2

The ℓ_1 error of EFM with fast algorithm in [19] for multiple choices of N and M .

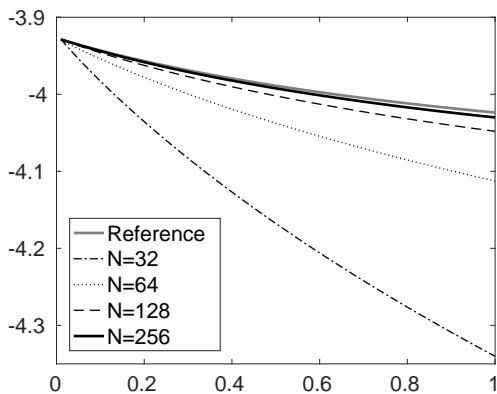


FIG. 3. The evolution of the entropy of EFM for multiple N values.

In order to demonstrate that the proposed method satisfies the H-theorem numerically, we define a time-dependent discrete entropy function

$$(4.14) \quad \eta(t) = \left(\frac{2T}{N}\right)^d \sum_{q \in X} F_q(t) \ln F_q(t).$$

The evolution of the entropy, plotted in Figure 3, shows that as the number of the discrete points N increases the discrete entropy converges to the one of the exact solution.

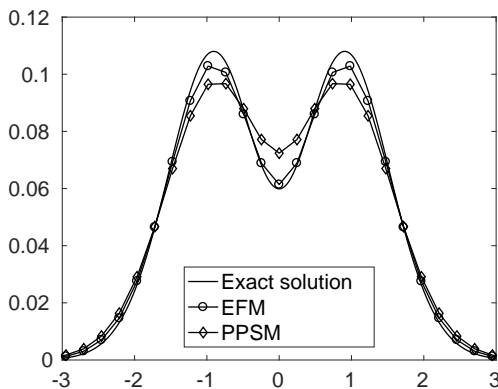


FIG. 4. Comparison between PPSM and EFM at time $t = 1$ with $N = 64$ for BKW solution.

As a comparison with PPSM, Figure 4 presents the numerical solutions in the v_1 direction of PPSM and EFM at $t = 1$ with $N = 32$. The smoothing filter used for EFM results in much less dissipation, thus leading to a much better agreement with the exact solution. Finally, Figure 5 shows that as N increases the solution of EFM converges rapidly to the exact solution.

Example 2 (Bi-Gaussian initial value). Another frequent example is a problem with the bi-Gaussian initial value

$$(4.15) \quad f(t = 0, v) = \frac{1}{4\pi} \left(\exp\left(-\frac{|v - u_1|^2}{2}\right) + \exp\left(-\frac{|v - u_2|^2}{2}\right) \right),$$

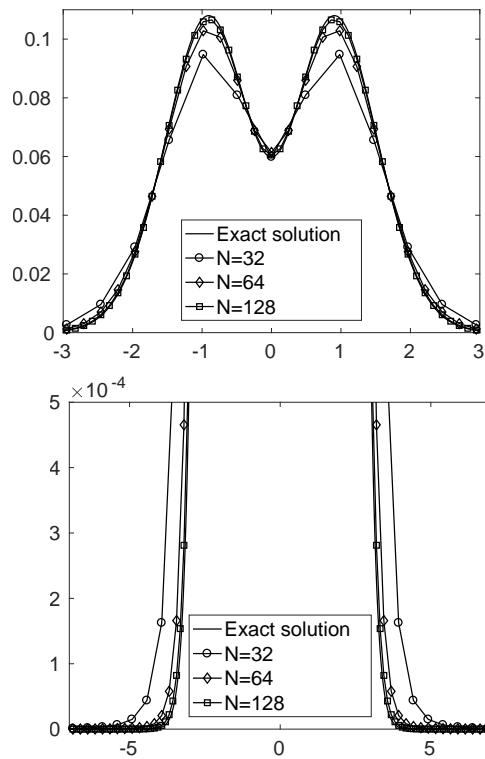


FIG. 5. Numerical solution of EFM for multiple N values with the BKW solution at time $t = 1$ on different scales.

where $u_1 = (-2, 0)^\top$ and $u_2 = (2, 0)^\top$. This is solved for the Maxwell molecules (2D in velocity) with radius $R = 6$. Figure 6 shows the numerical results of PPSM and EFM. The reference solution is calculated by the Fourier spectral method with $N = 400$ and $R = 8$. It is clear that EFM solution is much closer to the reference solution. Figure 7 demonstrates that as N increases EFM converges rapidly to the reference solution.

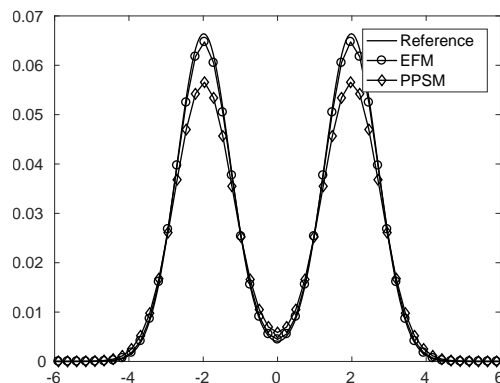


FIG. 6. Comparison between PPSM and EFM at $t = 1$ with $N = 64$ for the bi-Gaussian initial value.

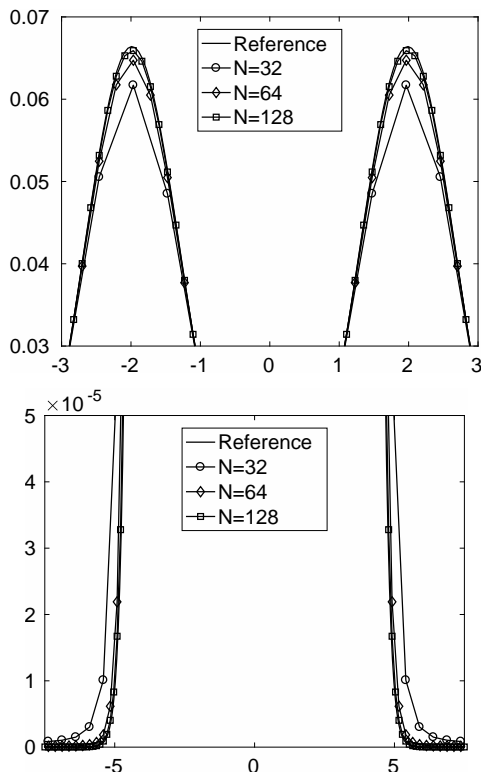


FIG. 7. Numerical solution of EFM for multiple N values with the bi-Gaussian initial value at time $t = 1$ on different scales.

Example 3 (Discontinuous initial value)... The initial condition given by

$$(4.16) \quad f(t = 0, v) = \begin{cases} \frac{\rho_1}{2\pi T_1} \exp\left(-\frac{|v|^2}{2T_1}\right), & \text{if } v_1 > 0, \\ \frac{\rho_2}{2\pi T_2} \exp\left(-\frac{|v|^2}{2T_2}\right), & \text{if } v_1 < 0, \end{cases}$$

in this example is discontinuous. Here $\rho_1 = \frac{6}{5}$ and the values of ρ_2 , T_1 and T_2 are uniquely determined by the three conditions

$$\int_{\mathbb{R}^2} f(0, v) dv = \int_{\mathbb{R}^2} f(0, v) |v|^2 / 2 dv = 1, \quad \int_{\mathbb{R}^2} f(0, v) v dv = 0.$$

The profile of the reference solution is presented in Figure 8, which is computed by EFM with $N = 2048$. Due to the discontinuity in the initial value, the spectral accuracy of FGM is lost. In addition, the Gibbs phenomenon leads to oscillations in the initial value of FGM. In Figure 9, the plots around the discontinuity demonstrate that EFM has a much better agreement as compared to FGM. The oscillations in FGM solutions exhibit large errors and the amplitude of the oscillation decreases slowly as N increases. On the contrary, there is no oscillation for EFM around the discontinuity and the solution is always kept non-negative.

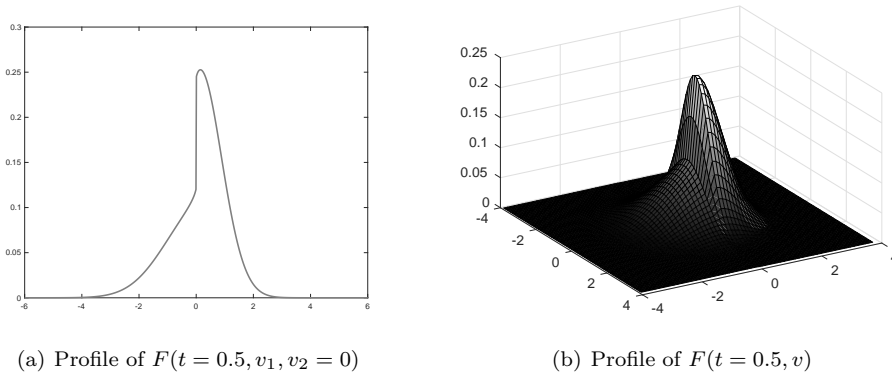


FIG. 8. Profile of $F(t, v)$ with the discontinuous initial value (4.16) at time $t = 0.5$.

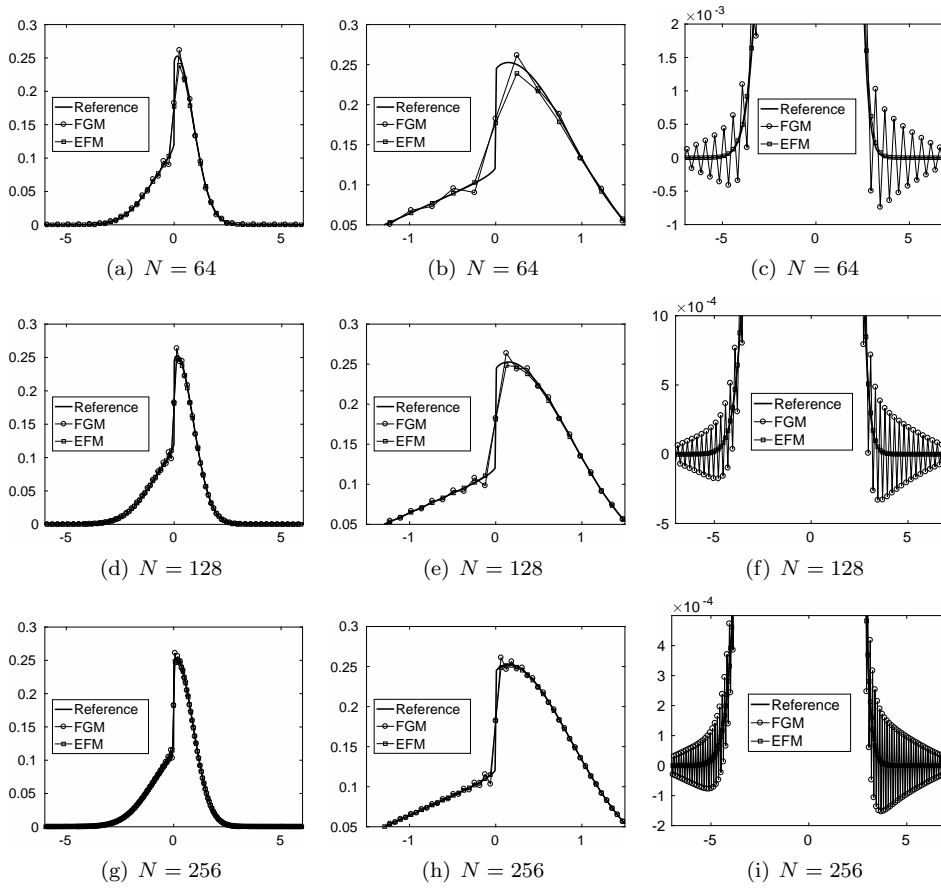


FIG. 9. Numerical solution of EFM and FGM for multiple N values with the discontinuous initial value (4.16) at time $t = 0.5$ on different scale.

Example 4 (3D BKW solution). The solution of this example is the exact 3D BKW solution, given by

$$(4.17) \quad f(t, v) = \frac{1}{(2\pi S)^{3/2}} \exp\left(-\frac{|v|^2}{2S}\right) \left(\frac{5S-3}{2S} + \frac{1-S}{2S^2}|v|^2\right),$$

where $S = 1 - 2 \exp(-t/6)/5$. Similarly to the 2D case, we first check the accuracy of EFM. At time $t = 0.01$, the ℓ_1 , ℓ_2 and ℓ_∞ errors and the convergence rates are listed in the Table 3. Similar to the 2D case, the convergence rate is of the second order and the errors are rather small.

N	ℓ_1 error	rate	ℓ_2 error	rate	ℓ_∞ error	rate
16	4.08×10^{-3}		3.08×10^{-3}		3.56×10^{-3}	
32	1.42×10^{-3}	1.52	1.12×10^{-3}	1.47	1.26×10^{-3}	1.50
64	4.07×10^{-4}	1.80	3.29×10^{-4}	1.76	3.72×10^{-4}	1.76
128	1.08×10^{-4}	1.91	8.85×10^{-5}	1.90	1.00×10^{-4}	1.89

TABLE 3

The ℓ_1 , ℓ_2 and ℓ_∞ errors and convergence rates for the BKW solution at time $t = 0.01$ with $R = 6$.

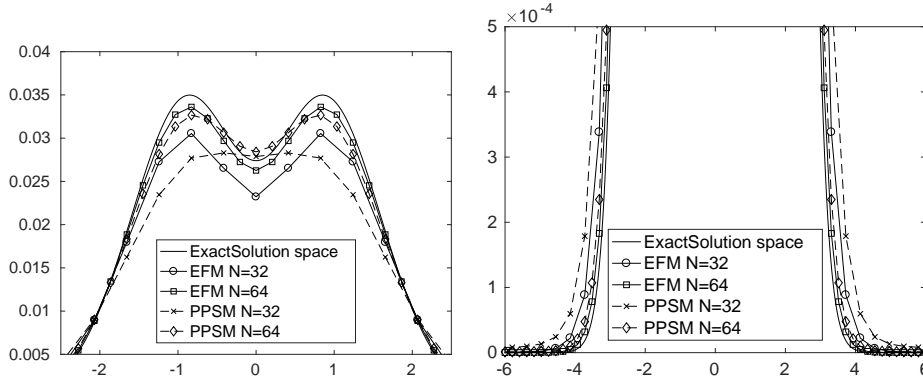


FIG. 10. Numerical solution of EFM and PPSM for multiple N values with the BKW solution at time $t = 1$ on different scales.

As a comparison with PPSM, Figure 10 presents the numerical solutions on the v_1 direction of PPSM and EFM at $t = 1$ with $N = 32$. The plots clearly show that the smoothing filter used in EFM results in much less dissipation, thus leading to a better agreement with the exact solution.

5. Discussion. EFM proposed in this paper is a trade-off between accuracy and preservation of physical properties. The resulting scheme can be viewed both as a discrete velocity method and a Fourier method. In terms of the convergence rate, it is better than DVM but slower than FGM. In terms of physical properties, it guarantees positivity, mass conservation and a discrete H-theorem, while the momentum and energy conservation is lost. Regarding the computational cost, fast algorithms in [19, 11] remain valid for EFM. As to the future work, we plan to study how to mitigate momentum and energy loss, where higher order accuracy is needed for long time simulation. The numerical implementation of the spatially inhomogeneous setting is also in progress.

Acknowledgments. The authors thank Jingwei Hu for discussion on the filter and fast algorithm on Boltzmann collision term.

REFERENCES

- [1] Jean-Marie Barbaroux, Dirk Hundertmark, Tobias Ried, and Semjon Vugalter. Gevrey smoothing for weak solutions of the fully nonlinear homogeneous boltzmann and kac equations without cutoff for maxwellian molecules. Archive for Rational Mechanics and Analysis, 225(2):601–661, Aug 2017.
- [2] G. A. Bird. Molecular Gas Dynamics and the Direct Simulation of Gas Flows. Oxford: Clarendon Press, 1994.
- [3] A. V. Bobylev. Exact solutions of the Boltzmann equation. In Akademiia Nauk SSSR Doklady, volume 225, pages 1296–1299, 1975.
- [4] A. V. Bobylev, A. Palczewski, and J. Schneider. On approximation of the Boltzmann equation by discrete velocity models. Comptes rendus de l’Académie des sciences. Série 1, Mathématique, 320(5):639–644, 1995.
- [5] A. V. Bobylev and S. Rjasanow. Difference scheme for the Boltzmann equation based on fast fourier transform. Technical report, 1996.
- [6] L. Boltzmann. Weitere studien über das wärmeleichgewicht unter gas-molekülen. Wiener Berichte, 66:275–370, 1872.
- [7] T. Carleman. Problemes mathématiques dans la théorie cinétique de gaz, volume 2. Almqvist & Wiksell, 1957.
- [8] G. Dimarco and L. Pareschi. Numerical methods for kinetic equations. Acta Numerica, 23:369–520, 2014.
- [9] L. Fainsilber, P. Kurlberg, and B. Wennberg. Lattice points on circles and discrete velocity models for the Boltzmann equation. SIAM Journal on Mathematical Analysis, 37(6):1903–1922, 2006.
- [10] F. Filbet and C. Mouhot. Analysis of spectral methods for the homogeneous Boltzmann equation. Transactions of the American Mathematical Society, 363(4):1947–1980, 2011.
- [11] I. M. Gamba, J. R. Haack, C. D. Hauck, and J. Hu. A fast spectral method for the Boltzmann collision operator with general collision kernels. SIAM Journal on Scientific Computing, 39(14):B658–B674, 2017.
- [12] I. M. Gamba and S. H. Tharkabhushanam. Spectral-lagrangian methods for collisional models of non-equilibrium statistical states. Journal of Computational Physics, 228(6):2012–2036, 2009.
- [13] D. Goldstein, B. Sturtevant, and J. E. Broadwell. Investigations of the motion of discrete-velocity gases. Progress in Astronautics and Aeronautics, 117:100–117, 1989.
- [14] S. Gottlieb, C. W. Shu, and E. Tadmor. Strong stability-preserving high-order time discretization methods. SIAM review, 43(1):89–112, 2001.
- [15] M. Krook and T. T. Wu. Exact solutions of the Boltzmann equation. The Physics of Fluids, 20(10):1589–1595, 1977.
- [16] G. G. Lorentz. APPROXIMATION OF FUNCTIONS (ATHENA SERIES). Holt, Rinehart and Winston New York, 1966.
- [17] G. Meinardus. Approximation of Functions: Theory and Numerical Methods. Springer, New York, 1967.
- [18] A. B. Morris, P. L. Varghese, and D. B. Goldstein. Improvement of a discrete velocity Boltzmann equation solver that allows for arbitrary post-collision velocities. In Rarefied Gas Dynamics: Proceedings of the 26th International Symposium, Kyoto, Japan, 2008.
- [19] C. Mouhot and L. Pareschi. Fast algorithms for computing the Boltzmann collision operator. Math. Comp., 75(256):1833–1852, 2006.
- [20] C. Mouhot, L. Pareschi, and T. Rey. Convolutional decomposition and fast summation methods for discrete-velocity approximations of the Boltzmann equation. ESAIM: Mathematical Modelling and Numerical Analysis, 47(5):1515–1531, 2013.
- [21] A. Palczewski, J. Schneider, and A. V. Bobylev. A Consistency Result for a Discrete-Velocity Model of the Boltzmann Equation. SIAM Journal on Numerical Analysis, 34(5):1865–1883, oct 1997.
- [22] A. V. Panferov and A. G. Heintz. A new consistent discrete-velocity model for the Boltzmann equation. Mathematical Methods in the Applied Sciences, 25(7):571–593, 2002.
- [23] L. Pareschi and B. Perthame. A fourier spectral method for homogeneous Boltzmann equations. Transport Theory and Statistical Physics, 25(3-5):369–382, 1996.
- [24] L. Pareschi and G. Russo. Numerical solution of the Boltzmann equation I: Spectrally accurate

- approximation of the collision operator. SIAM J. Numer. Anal., 37(4):1217–1245, 2000.
- [25] L. Pareschi and G. Russo. On the stability of spectral methods for the homogeneous Boltzmann equation. Transport Theory and Statistical Physics, 29(3-5):431–447, 2000.
- [26] T. Platkowski and R. Illner. Discrete velocity models of the Boltzmann equation: a survey on the mathematical aspects of the theory. SIAM review, 30(2):213–255, 1988.
- [27] F. Rogier and J. Schneider. A direct method for solving the Boltzmann equation. Transport Theory and Statistical Physics, 23(1-3):313–338, 1994.
- [28] S. Simons. Is the solution of the Boltzmann equation positive? Physics Letters A, 69(4):239 – 240, 1978.
- [29] P. L. Varghese. Arbitrary post-collision velocities in a discrete velocity scheme for the Boltzmann equation. In Proc. of the 25th Intern. Symposium on Rarefied Gas Dynamics/Ed. by MS Ivanov and AK Rebrov. Novosibirsk, pages 225–232, 2007.
- [30] A. Weiße, G. Wellein, A. Alvermann, and H. Fehske. The kernel polynomial method. Reviews of modern physics, 78(1):275, 2006.